

Electron Pair Production in the Field of the Proton and in the Field of the Electron by Photons of Energy from 10 Mev to 1 Bev*

E. L. HART,† G. COCCONI, V. T. COCCONI, AND J. M. SELLEN‡
Cornell University, Ithaca, New York

(Received March 12, 1959)

A 24-in. diffusion cloud chamber filled with hydrogen and located in a magnetic field has been placed in the hardened bremsstrahlung beam of the Cornell synchrotron to study electron pair production in the proton field (P.F. pairs) and in the electron field (E.F. pairs). The E.F. pairs could be detected with an average efficiency of $\sim 85\%$ and are about as abundant as the P.F. pairs. A total of 3065 pairs produced by photons with energy from 10 to 1040 Mev have been analyzed.

The principal results are:

- (1) The recoil momentum distribution of the E.F. pairs is in good agreement with the distribution predicted by Suh and Bethe.
- (2) The cross section for E.F. pairs is consistent with that calculated by Wheeler and Lamb.
- (3) The distribution of the opening angle of P.F. and E.F. pairs is in general agreement with Borsellino's calculations, at large angles. However, the peak appears at smaller angles than predicted.

I. INTRODUCTION

THE theory of the production of electron pairs in the field of the proton (hereafter called P.F. pairs) and in the field of the electron (hereafter called E.F. pairs) constitutes a conceptually well-established chapter of quantum electrodynamics. However, the formal complexity of the equations has often forced theorists to make simplifying assumptions or approximations that limit the validity of their results, or has discouraged them from working out in detail the quantities suitable for comparison with experiments.

One of the main difficulties in treating pair production in the light elements (in hydrogen in particular) is introduced by the screening correction. For photons between 20 Mev and 1 Bev one is in the region of intermediate screening (i.e., one can neither neglect it nor use the asymptotic approximations of complete screening).

Originally, the total cross section for the production of P.F. pairs was computed by Bethe and Heitler¹ with the screening correction based on the electron distribution of the Fermi-Thomas model. The best calculation now available is that by Wheeler and Lamb,² who have introduced the exact hydrogen wave functions to account for screening.

The total cross section for E.F. pair production was similarly calculated by Wheeler and Lamb,² again with the exact hydrogen wave functions. They assumed that for small recoil momenta the cross section for E.F. pairs is equal to that for P.F. pairs, while for large

recoil momenta the electron can be considered as free. These assumptions have now been quantitatively justified by Suh and Bethe³ for photon energies larger than 100 Mev.

Borsellino⁴ has developed a general equation that describes the differential cross section for E.F. pair production as a function of all the parameters involved. This calculation does not contain the screening correction and omits the exchange terms as well as the so-called γ - e interaction terms.⁵ The equation is therefore valid for all recoil momenta for which screening is not important, as long as the recoil energy is much smaller than the photon energy. Practically all the information useful for comparison with experiments on E.F. pairs is implicit in Borsellino's equation, but its extraction requires painful calculations.

One of the most interesting points of comparison between experiment and theory is the momentum distribution of the recoil electrons of the E.F. pairs. A detailed calculation of this distribution was made by Votruba,⁶ who solved the problem for a free electron exactly, but with the condition that the recoil momenta be small compared with mc . His results are thus valid only for a very small range of recoil momenta between mc and some smaller value at which screening becomes important for the particular photon energy considered. In the accompanying paper, Suh and Bethe extract from Borsellino's equation a distribution of the recoil momentum for photon energies above 100 Mev, which is valid over the much wider range of recoil momenta where Borsellino's equation applies.

Another theoretical result to be compared with experiments is the distribution of the opening angle

* Work supported in part by the joint program of the Office of Naval Research and the U. S. Atomic Energy Commission.

† This paper is based on a thesis submitted to the Graduate School of Cornell University in partial fulfillment of the requirements for a Ph.D. degree.

‡ Now at the Ramo-Wooldridge Corporation, Los Angeles, California.

¹ H. A. Bethe and W. Heitler, Proc. Roy. Soc. London **A146**, 83 (1934).

² J. A. Wheeler and W. E. Lamb, Phys. Rev. **55**, 858 (1939), and **101**, 1836(E) (1956).

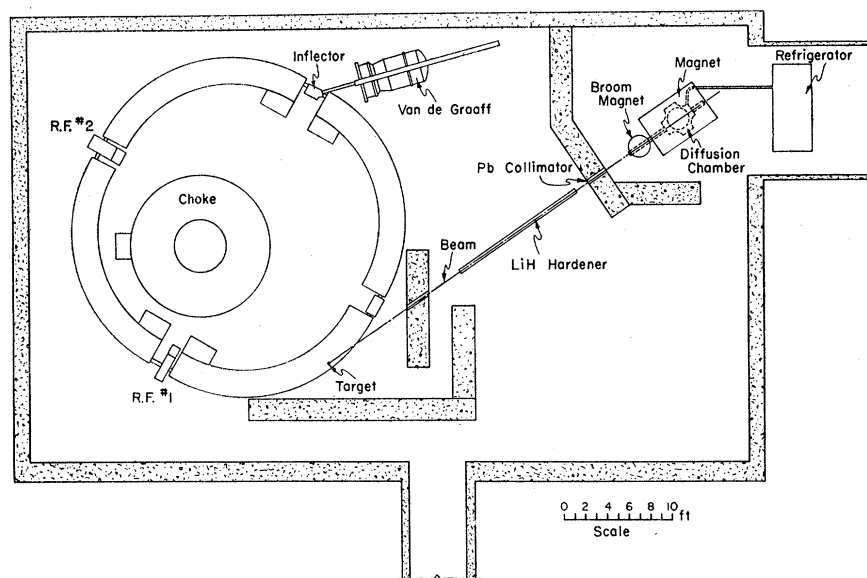
³ K. S. Suh and H. A. Bethe, preceding paper [Phys. Rev. **115**, 672 (1959)].

⁴ A. Borsellino, Rev. univ. nacl. Tucumán Ser. A, **6**, 7 (1947).

⁵ See the review paper by J. Joseph and F. Rohrlich, Revs. Modern Phys. **30**, 354 (1958).

⁶ V. Votruba, Phys. Rev. **73**, 1468 (1948).

FIG. 1. General layout of the experiment.



between the members of the electron pairs. This has been computed for P.F. pairs by Borsellino.⁷

Experimental verification of the theoretical results is, so far, scanty, as only recently have photon sources of high energy been developed, as well as suitable hydrogen targets and detectors capable of distinguishing between P.F. pairs and E.F. pairs.

Several measurements of the total cross sections for pair production at photon energies $E_\gamma < 300$ Mev, and one at 2.5 Bev are reported in the literature. An experiment at $E_\gamma = 1$ Bev is described in the accompanying paper by Malamud⁸ (see that paper for a survey of the literature on this subject). In all these experiments the sum of the cross sections for P.F. and E.F. pair production was measured and the partial cross sections were deduced by assuming that P.F. pair production is correctly described by the Bethe-Heitler or the Wheeler and Lamb formulas.

As far as other details of the processes are concerned, only very meager information is available for $E_\gamma < 300$ Mev and practically nothing at higher photon energies.⁵

Presently, Anderson *et al.*⁹ are studying P.F. and E.F. pair production in a 4-in. hydrogen bubble chamber using the 300-Mev electron synchrotron at Berkeley.

The present work is a study of the processes of pair production both in the proton field and in the electron field by photons with energies between 10 Mev and 1 Bev, in the hydrogen gas of a diffusion cloud chamber. Measurements have been made of (1) the momentum distribution of the recoil electron of E.F. pairs, (2) the angular distribution of the recoil electron, (3) the P.F. and E.F. pair cross sections as a function

of the photon energy, (4) the opening angle of both P.F. and E.F. pairs, and (5) the energy-sharing between the pair members.

Hydrogen is used as a target to maximize the ratio of E.F. pairs to P.F. pairs. As this ratio is roughly equal to $1/Z$, in H_2 about as many E.F. pairs are produced as P.F. pairs.

In order to study E.F. pairs, one has to detect and if possible measure the momentum of the recoil electron in whose field the pair was created. As the majority of these recoils have momenta smaller than mc , it is essential that the H_2 target be such as to make the recoil range as long as possible.

The diffusion cloud chamber with magnetic field meets the above requirement of providing a dilute H_2 target, and supplies detailed information on the kinematics of the individual events. Its usual drawback, the small depth of its sensitive layer, is of no concern here provided the photon beam is passed through the chamber at midheight of its sensitive region. The small opening angle characteristic of the electromagnetic processes confines the tracks to a region much shallower than the sensitive layer, allowing one to take advantage of the full size of the chamber when making curvature measurements.

The proton recoil of P.F. pairs in general does not acquire sufficient momentum to make even a grain. In the ~ 1500 P.F. pairs analyzed only one proton recoil was observed, which is consistent with the theoretical predictions of Suh and Bethe.

II. APPARATUS

The bremsstrahlung beam of the Cornell synchrotron (peak energy 1040 Mev), hardened by ~ 2.6 radiation lengths of lithium hydride and collimated to a ribbon $\frac{3}{4}$ in. wide and $\frac{3}{16}$ in. high, was used as the photon source.

⁷ A. Borsellino, *Phys. Rev.* **89**, 1023 (1953).

⁸ H. Malamud, following paper [*Phys. Rev.* **115**, 687 (1959)].

⁹ J. D. Anderson *et al.*, private communication and *Bull. Am. Phys. Soc. Ser. II*, **1**, 376 (1956).

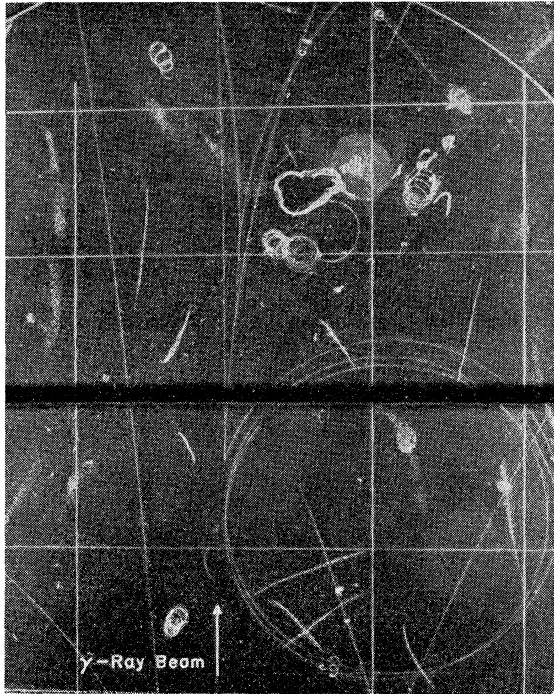


FIG. 2. Examples of events observed in the cloud chamber. The event in the upper half of the picture is a pair produced in the field of a proton by a photon of 97 Mev. The other event is a pair produced by a photon of 620 Mev in the field of an electron which recoils with a momenta of 9.8 Mev/c.

The diffusion cloud chamber was filled with H_2 at 18 atmos, and operated in a magnetic field of 5.4 kilogauss. The sensitive layer (24 in. across, 3 in. high) was photographed by a stereoscopic camera (Fig. 1).¹⁰

The beam intensity was adjusted to produce in the chamber gas from 1 to 2 electron pairs per picture. Only events whose origin lay in a restricted region at the center of the chamber were considered. The track length of almost all pair members was greater than 25 cm. Scanning efficiency was practically 100%. Contaminations due to the presence of the methyl alcohol vapor in the chamber introduced a correction of $\sim 1.5\%$. The correction for the possibility that a Compton electron originates close enough to a pair to simulate the recoil of an E.F. pair was found to be negligible ($\sim 0.1\%$).

For the analysis, all events were reprojected in space to measure angles and momenta. The techniques used are described in the appropriate sections.

Figure 2 shows an example of a P.F. pair and of an E.F. pair whose recoil electron has a momentum $q_R = 9.8$ Mev/c.¹¹

As mentioned in the introduction, the critical point of any experiment of this kind is the distinction between

¹⁰ The effect of the LiH hardener is discussed in the Appendix. A more detailed description of the apparatus may be found in Sellen, Cocconi, Cocconi and Hart, Phys. Rev. **113**, 1323 (1959).

¹¹ Following the usual convention, the electron with the lower momentum is defined as the recoil.

P.F. pairs and E.F. pairs, which depends upon the detection of the recoil electron of the E.F. pairs. With decreasing recoil momentum, the recoil track appears as a tight helix, a blob, a grain, or not at all.

In our chamber (H_2 density at beam height 0.017 g/cm³), an electron with recoil momentum $q_R = 0.15$ Mev/c (25-kev kinetic energy) has a range of 3 mm and is deflected by the magnetic field through an angle π . We define this to be our "minimum measurable momentum." However, recoils with a momentum as low as 0.02 Mev/c (400 ev kinetic energy) still produce a recognizable grain at the origin, identifying the event as an E.F. pair. We define $q_R = 0.02$ Mev/c as our "minimum detectable momentum."¹²

Accordingly, we shall call "experimental triplets" all the E.F. pairs with detectable recoil ($q_R \geq 0.02$ Mev/c), which constitute about 85% of all E.F. pairs (See Sec. 4). The other events, which include all the P.F. pairs plus that 15% of the E.F. pairs whose recoil is invisible, shall be called "experimental pairs."

A group of pictures fully analyzed yielded 1537 experimental pairs and 1227 experimental triplets. To improve the statistics on E.F. pairs, 301 additional triplets with measurable momentum were extracted from another group of pictures in which the pairs were not measured.

III. MOMENTUM DISTRIBUTION OF THE RECOIL ELECTRONS OF E.F. PAIRS

Among the experimental triplets examined, 954 had recoil electrons of measurable momentum ($q_R \geq 0.15$ Mev/c). For these events the recoil momentum was measured by using the following techniques:

Recoil momenta between 0.15 and 0.20 Mev/c were determined from the track range, with an error $< 15\%$. Momenta between 0.2 and 1.0 Mev/c were determined by measuring the pitch and diameter of the envelope of the helix described by the track and were checked by measuring the range whenever possible. Depending on the dip angle, the error in q_R was between 5 and 10%. Recoils of higher momentum, which are generally emitted at small angles to the photon direction, could be fitted to templates and their momenta measured with an error $< 5\%$.

The experimental momentum distributions are given in Fig. 3 for three photon energy intervals. The solid line in each figure is the distribution calculated by Suh and Bethe from Borsellino's equation, normalized at $q_R = 0.4$ Mev/c.

For $E_\gamma > 100$ Mev the experimental distributions appear to be practically independent of photon energy,

¹² This value was estimated by counting the number of recognizable δ -rays along tracks of positrons with energy greater than 100 Mev. An average of 0.7 δ -rays/cm were found, which, according to Bhabha's formula, indicates that electrons with momentum as low as 0.02 Mev/c can be detected. The number of E.F. pairs with recoil momentum between 0.15 Mev/c and 0.02 Mev/c was decreased by 5% to compensate for the P.F. pairs which have a δ -ray close enough to the origin to make them appear as E.F. pairs.

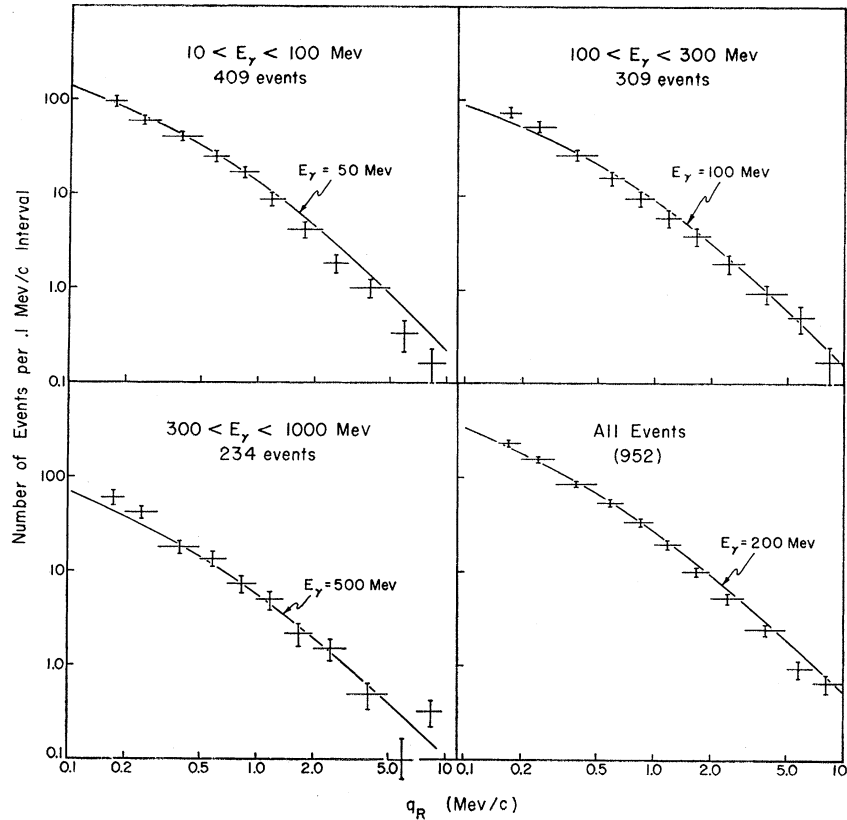


FIG. 3. Distribution of the recoil momentum q_R acquired by the electron in whose field the pair production has occurred. The first three distributions refer to the events having primary photon energy, E_γ , in the indicated range. The last contains all the events, irrespective of photon energy. The solid curves are the distributions calculated by Suh and Bethe for the indicated photon energies. The curves are normalized to the experimental distributions at $q_R=0.4$ Mev/c.

as predicted by Suh and Bethe. The over-all agreement between experiment and theory is remarkably good.

Although the approximations used in the theory become invalid as the photon energy falls below 100 Mev, the experimental results in the range $10 < E_\gamma < 100$ Mev are compared with the theoretical curve for $E_\gamma=50$ Mev. The experimental points fit the curve well up to $q_R \approx 1$ Mev/c, then seem to fall below by an increasing amount as the recoil momentum becomes larger. This can be attributed (a) to exchange effects, neglected in the theory, which become important in this region, and (b) to the increasing fraction of the available energy that must be given to the recoil.

In the figure, only recoil momenta up to 10 Mev/c have been plotted. Actually 16 events were found with $q_R > 10$ Mev/c. The maximum recoil momentum observed was 139 Mev/c with a primary photon of 760 Mev.

IV. CROSS SECTION FOR E.F. PAIR PRODUCTION

The knowledge of the total number of E.F. pairs with recoil momentum $q_R \geq q_{\min}$ permits an estimate of the cross section for production of E.F. pairs with recoil momentum larger than that minimum, $\sigma_{E.F.}(q_R \geq q_{\min})$.

Let ρ be the ratio of the observed number of experimental triplets with $q_R \geq q_{\min}$ to the total number of events (pairs+triplets) observed in a given interval of

photon energy. Then

$$\sigma_{E.F.}(q_R \geq q_{\min}) = \rho(\sigma_{E.F.} + \sigma_{P.F.}),$$

where $\sigma_{E.F.}$ and $\sigma_{P.F.}$ are the average cross sections for the production of E.F. and P.F. pairs, respectively, in the photon energy interval considered.

In Table I are given the experimental values of ρ for $q_{\min}=0.02$ Mev/c (the minimum detectable momentum) and for $q_{\min}=0.15$ Mev/c (the minimum measurable momentum).

The two solid curves in Fig. 4 are the cross sections $\sigma_{E.F.}$ and $\sigma_{P.F.}$ (in units of αr_0^2) as deduced from the equations of Wheeler and Lamb, and adjusted to take into account the effect of molecular binding in hydrogen.¹³ With these curves and the values of ρ given in

TABLE I. Values of the ratio ρ between the number of observed E.F. pairs with $q_R \geq q_{\min}$ and the total number of events observed, for the indicated intervals of photon energies. The first row includes all events with $q_R \geq 0.15$ Mev/c, the minimum measurable momentum; the second, all events with $q_R \geq 0.02$ Mev/c, the minimum detectable momentum.

\bar{E}_γ (Mev)	35	75	150	300	600	900
ρ (0.02 Mev/c)	0.512 ± 0.038	0.462 ± 0.035	0.465 ± 0.032	0.425 ± 0.031	0.391 ± 0.032	0.424 ± 0.069
ρ (0.15 Mev/c)	0.334 ± 0.032	0.244 ± 0.026	0.233 ± 0.023	0.197 ± 0.022	0.198 ± 0.024	0.246 ± 0.054

¹³ D. Bernstein and W. K. H. Panofsky, Phys. Rev. **102**, 522 (1956).

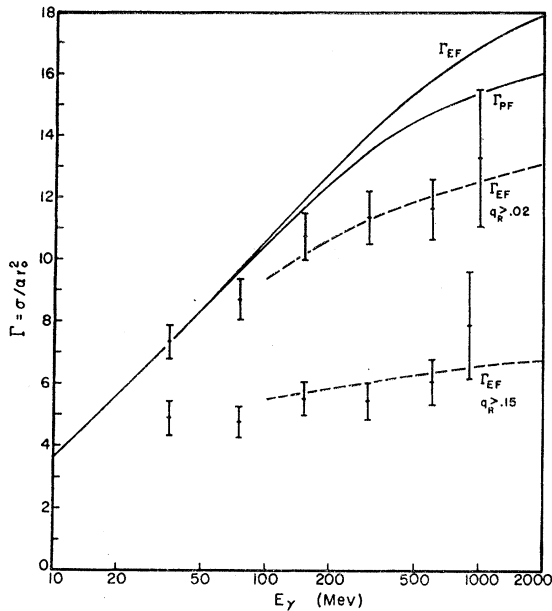


FIG. 4. The two sets of experimental points represent the energy dependence of the partial cross section for the production of E.F. pairs with recoil momentum greater than 0.02 and 0.15 Mev/c, respectively. The solid curves are the total cross sections $\sigma_{P.F.}$ and $\sigma_{E.F.}$ calculated by Wheeler and Lamb. The experimental points for $\sigma_{E.F.}(q_R \geq 0.15 \text{ Mev}/c)$ are compared to the cross section calculated by Suh and Bethe for the same range of recoil momenta (lower dashed curve). The points for $\sigma_{E.F.}(q_R \geq 0.02 \text{ Mev}/c)$ are compared with the results (upper dashed curve) obtained by adding Suh and Bethe's cross section for $q_R \geq 0.05 \text{ Mev}/c$ to the cross section calculated by Votruba for $0.02 < q_R < 0.05 \text{ Mev}/c$. All the cross sections are expressed in units of $\alpha r_0^2 = 5.793 \times 10^{-28} \text{ cm}^2$.

the table, one obtains the two sets of points for $\sigma_{E.F.}(q_R \geq q_{\min})$ plotted in the figure.

In the region $100 \text{ Mev} < E_\gamma < 1 \text{ Bev}$ the results for $\sigma_{E.F.}(q_R \geq 0.15 \text{ Mev}/c)$ may be directly compared with the prediction of Suh and Bethe (lower dashed line in the figure). The agreement is satisfactory.

The approximations introduced in Suh and Bethe's calculation are not valid below $q_R \approx 0.05 \text{ Mev}/c$. The points for $\sigma_{E.F.}(q_R \geq 0.02 \text{ Mev}/c)$ are therefore compared with the cross section (upper dashed curve) obtained by adding to Suh and Bethe's cross section for $q_R \geq 0.05 \text{ Mev}/c$ the cross section given by Votruba⁶ for $0.02 < q_R < 0.05 \text{ Mev}/c$. Once again, the agreement is reasonably good.

Neither Votruba's nor Suh and Bethe's calculations take screening into account, but for the energies and recoil momenta considered here the screening correction is negligible.

For photon energies $E_\gamma < 100 \text{ Mev}$ there are no theories available, and the experimental points may be used to extend Suh and Bethe's curve.

It is worth pointing out that the experimental results on $\sigma_{E.F.}$ indicate that practically all the E.F. pairs produced by photons with $E_\gamma < 50 \text{ Mev}$ could be distinguished from P.F. pairs in our chamber, and that

for $E_\gamma = 1 \text{ Bev}$ about 75% of the E.F. pairs could still be detected.¹⁴ It is estimated that averaging over the range of photon energies from 10 Mev to 1 Bev, our efficiency for detecting recoil electrons was $\sim 85\%$.

In the region $E_\gamma < 100 \text{ Mev}$, where most of the E.F. pairs can be detected, the absolute value of $\sigma_{E.F.}$ can be determined using only the assumption that P.F. pair production is correctly described by the Wheeler and Lamb cross section. The results obtained are the following:

(a) For $10 < E_\gamma < 50 \text{ Mev}$, $\bar{\sigma}_{E.F.} = 4.11 \pm 0.55 \text{ mb}$, to be compared with the Wheeler and Lamb value $\bar{\sigma}_{E.F.} = 4.06 \text{ mb}$.

(b) For $50 \text{ Mev} < E_\gamma < 100 \text{ Mev}$, $\bar{\sigma}_{E.F.} = 4.55 \pm 0.71 \text{ mb}$ while the theory gives $\bar{\sigma}_{E.F.} = 5.60$.

V. ANGULAR DISTRIBUTION OF THE RECOIL ELECTRONS OF E.F. PAIRS

The emission angle, θ_R , of the recoil electron relative to the photon direction was determined for all 954 triplets with measurable recoil momentum by measuring the projected emission angle and the dip angle of the recoil. The error in the determination of θ_R is generally smaller than 5° .

The scatter diagram of Fig. 5 gives the distribution

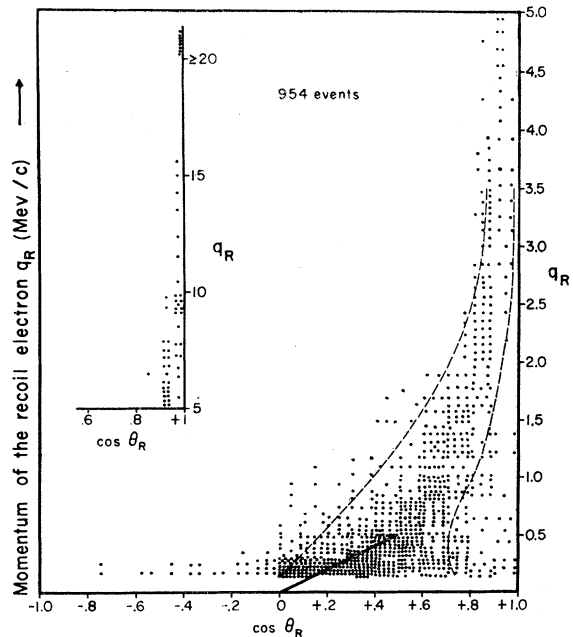


FIG. 5. Each dot in the figure corresponds to an E.F. pair whose recoil electron has momentum q_R , and is emitted at an angle θ_R . All events are included, irrespective of the primary photon energy. The short straight line at the bottom of the figure is the distribution expected in first approximation for $q_R < mc$. The two dashed lines are the 10th and 90th percentile of the data. The few events corresponding to negative values of $\cos \theta_R$ are justified in the text.

¹⁴ The efficiency for detection of E.F. pair recoils increases with decreasing photon energy since the minimum possible recoil momentum is $\sim 2mc(mc^2/E_\gamma)$.

of the recoil angle, $\cos\theta_R$ vs the recoil momentum q_R . The events have been plotted irrespective of the photon energy since the recoil angular distribution, like the momentum distribution, appears to be independent of the photon energy.

No detailed comparison with theory is possible here, as no one has yet ventured to extract this information from Borsellino's equation. However, the general shape of the distribution is determined by the fact that the transverse momentum of the recoil is of the order of mc , hence high-momentum recoils are emitted mostly forwards while recoils of low momenta appear at large angles.

From simple arguments of energy and momentum conservation, it can be shown that under the conditions $q_R < 0.5 \text{ Mev}/c$ and $E_\gamma \gg mc^2$,

$$\cos\theta_R \approx q_R/2mc.$$

In Fig. 5, the dots appear to concentrate along the line that represents the above function. It is interesting to note the lacuna in the region of small angles and moderate momenta.

The recoil electron cannot be emitted backwards if the pair is produced in the field of a free electron. However, a *bound* electron may occasionally recoil backwards when the momentum it acquires is small. Furthermore, scattering of the recoil electron by the protons of the molecule in which the pair was produced may account for some large backward emission angles. The scatter diagram contains 28 recoil electrons, all with low momenta, that have emission angles greater than 90° . For 12 cases θ_R is larger than 100° . The measurement uncertainty can account only for some cases, close to 90° .

VI. ENERGY PARTITION BETWEEN THE ELECTRON AND POSITRON IN P.F. AND E.F. PAIRS

The energy partition between the members of the created pair is generally expressed in terms of the energy imparted to the positron, E^+ , relative to the total energy of the pair, $E^+ + E^-$; i.e.,

$$f = E^+ / (E^+ + E^-).$$

Several accurate determinations of the distribution of f have been published (for the literature see the accompanying paper by Malamud⁸) in the energy range $E_\gamma \leq 300 \text{ Mev}$ for target materials with $Z > 13$, hence for events that are in the great majority pairs produced in the field of the nucleus. All the available results indicate good agreement with the theory of Bethe and Heitler. The same general conclusion is reached by Malamud for pairs produced in Be by photons of 1 Bev. However, to our knowledge there is no direct verification of the theory in H_2 , i.e., for pairs produced either in the field of the proton or in the field of the electron.

For the events observed in our pictures, the energy partition can be directly determined by measuring the momenta of the pair members. In general, the pair

members, being emitted with small dip angles (usually less than 5° for momenta greater than $10 \text{ Mev}/c$), lie in a plane practically normal to the magnetic field and their momenta can be measured with templates in that plane. The error is smaller than 5% for momenta from $10 \text{ Mev}/c$ to $500 \text{ Mev}/c$ (curvature $\sim 3.5 \text{ m}$) and is 5 to 10% for higher momenta. For momenta smaller than a few Mev/c the techniques described in Sec. 3 were used.

On the left-hand side of Fig. 6 are plotted the f -distributions for the 1524 experimental triplets produced by photons with energy in the three indicated intervals. In each of these figures the scale of the abscissa is chosen to make the Wheeler and Lamb² f -distribution a horizontal line instead of the familiar "inverted ω " of the plots with linear abscissas.

Similar plots for the 1534 experimental pairs were found to agree reasonably well with the expected distributions. Since the theoretical predictions for the f -distributions for P.F. and E.F. pairs are almost identical, the two groups of experimental data have been plotted together to improve the statistics (right-hand side of Fig. 6). The agreement is reasonable.

VII. OPENING ANGLE BETWEEN PAIR MEMBERS OF P.F. AND E.F. PAIRS

The most probable opening angle of an electron-positron pair produced in the field of either a proton or an electron by a photon of energy E_γ is $\sim 4mc^2/E_\gamma$, i.e., $\sim 2^\circ$ for $E_\gamma = 50 \text{ Mev}$, and $\sim \frac{1}{5}^\circ$ for $E_\gamma = 500 \text{ Mev}$.

The projection of the opening angle on a plane normal to the magnetic field was measured for 1320 experimental triplets and 1051 experimental pairs. The technique used was the following: The two templates that match the curvature of the positron and the electron are superimposed on the tracks of the pair members so that they extend beyond the origin, and a circular protractor centered at the event origin is placed on top of the templates. The projected opening angle, ω' , is then given by $\omega' = (\alpha_1 - \alpha_2)/2$, where α_1 and α_2 are the arcs intersected by the templates on the protractor, in front of and behind the event. The measurement error has been determined to be generally smaller than $\frac{1}{4}^\circ$.

For P.F. pairs, our results can be compared with Borsellino's calculation.¹⁵ For E.F. pairs there is no

¹⁵ We take this opportunity to correct some misprints in Borsellino's paper (reference 7). 1. In Eq. (6), the expression for F_2 should have the third term in the first parenthesis divided by 2, and in the expression for F_3 the exponents of the two Q 's must be interchanged. It should therefore read:

$$F_2 = \frac{1}{6} \left(16 + \frac{21}{Q^2} - \frac{17}{2Q^4} \right) L - \frac{1}{12} \left(28 + \frac{17}{Q^2} \right) \Delta,$$

$$F_3 = \frac{1}{2} \left(4 - \frac{1}{Q^4} \right) L - \frac{1}{2} \left(2 + \frac{1}{Q^2} \right) \Delta.$$

2. In the caption to Fig. 3 the statement after the last semicolon should be deleted. We thank Mr. R. M. Schectman of our laboratory for pointing out these misprints, and Dr. Borsellino for discussing them with us at length.

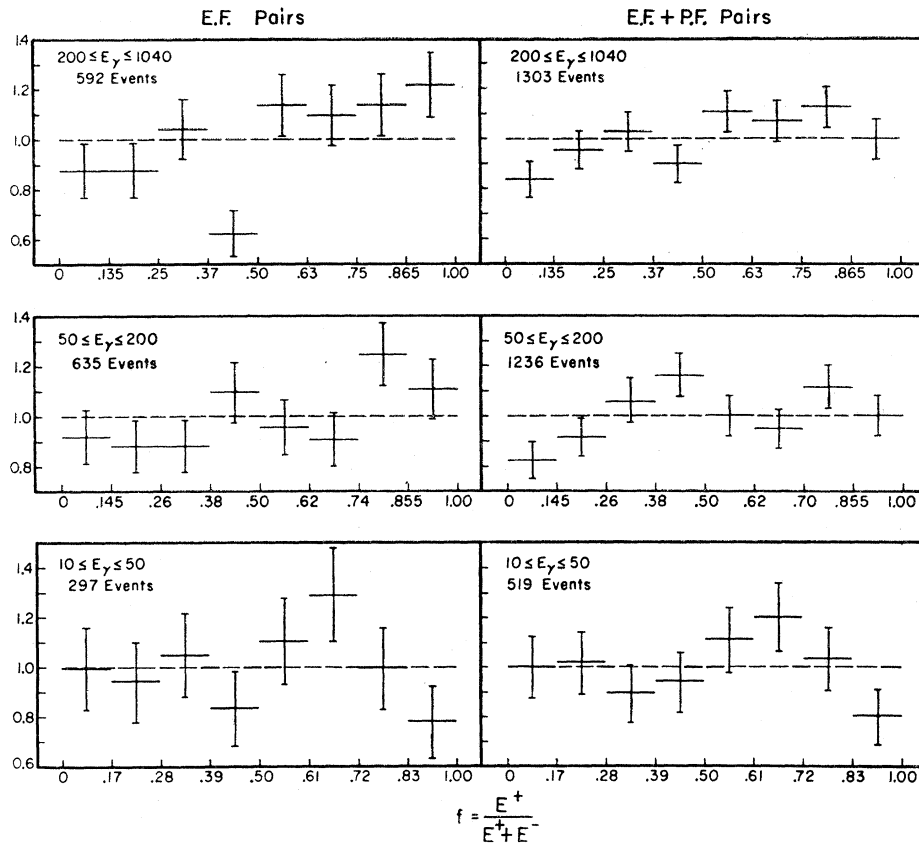


FIG. 6. Energy partition between the members of electron pairs, expressed in terms of the ratio $f = E^+ / (E^+ + E^-)$. The left-hand side of the figure refers to E.F. pairs, the right-hand side to all events, (E.F. + P.F.) pairs, observed in the indicated interval of photon energies. The scales of the abscissas are such that the f -distribution calculated by Wheeler and Lamb² is a horizontal line (dashed line in each figure). The experimental points are normalized to it.

theoretical prediction available, but it is reasonable that the opening angles should be much the same as for P.F. pairs, as long as the electron recoil energy is small.

In order to compare Borsellino's results with our data, we have (a) deduced from his formulas the distribution of the projected opening angle ω' , and (b) folded in an angular resolution of $\pm \frac{1}{4}^\circ$.

No meaningful difference was observed in the results obtained for experimental pairs and triplets. All the events were therefore grouped together in the final plots. Figure 7 gives the results for two photon energy groups. Each group is subdivided into two subgroups of roughly even, and uneven energy-sharing.

Following Borsellino, the scale of the abscissa is

TABLE II. Median values of the parameter $x = \omega / \omega_0$, where ω is the space opening angle of electron pairs, and $\omega_0 = mc^2 E_\gamma / E^+ E^-$. The first and second columns give the experimental results obtained from the cloud chamber data and from the data of Baroni *et al.*^a The third column gives the values deduced from Borsellino's theory.^b The two rows are for approximately even, and uneven energy-sharing between the pair members.

	Cloud chamber	Median x Baroni <i>et al.</i>	Borsellino's theory
Even energy-sharing	1.31 ± 0.05	1.20 ± 0.12	1.50
Uneven energy-sharing	1.00 ± 0.05	...	1.10

^a See reference 16.

^b See reference 7.

$x' = \omega' / \omega_0$, where $\omega_0 = mc^2 E_\gamma / E^+ E^-$. The spread in x' due to the $\frac{1}{4}^\circ$ angular resolution is indicated in each figure. Folding this resolution in the theoretical curves hardly modifies them, except at small x' .

The agreement between our data and the theory is satisfactory for $x' > \sim 1.5$. As predicted by the theory, the x' distributions for the events with uneven energy sharing are displaced toward smaller x' relative to the distributions for the events with even sharing.

For $x' < \sim 1.5$, however, the experimental points appear to peak to the left of the theoretical curves for all the groups of events considered. A similar discrepancy was observed by Baroni *et al.*¹⁶ for 107 electron pairs produced in photographic emulsion by cosmic rays of mean energy $\bar{E}_\gamma = 100$ Mev, and having $0.25 < f < 0.75$.

In Table II are given the median values of the parameter x for approximately even and uneven energy sharing, as deduced from our results, from the results of Baroni *et al.*, and from Borsellino's calculation. Here, x is a function of the true space opening angle ω . The experimental results lie 10 to 20% below the theoretical values.

A useful number for experimenters is the median value of the quantity $\phi = \omega E_\gamma / 4mc^2$, which allows an

¹⁶ Baroni, Borsellino, Scarsi, and Vanderhaeghe, *Nuovo cimento* **10**, 1653 (1953).

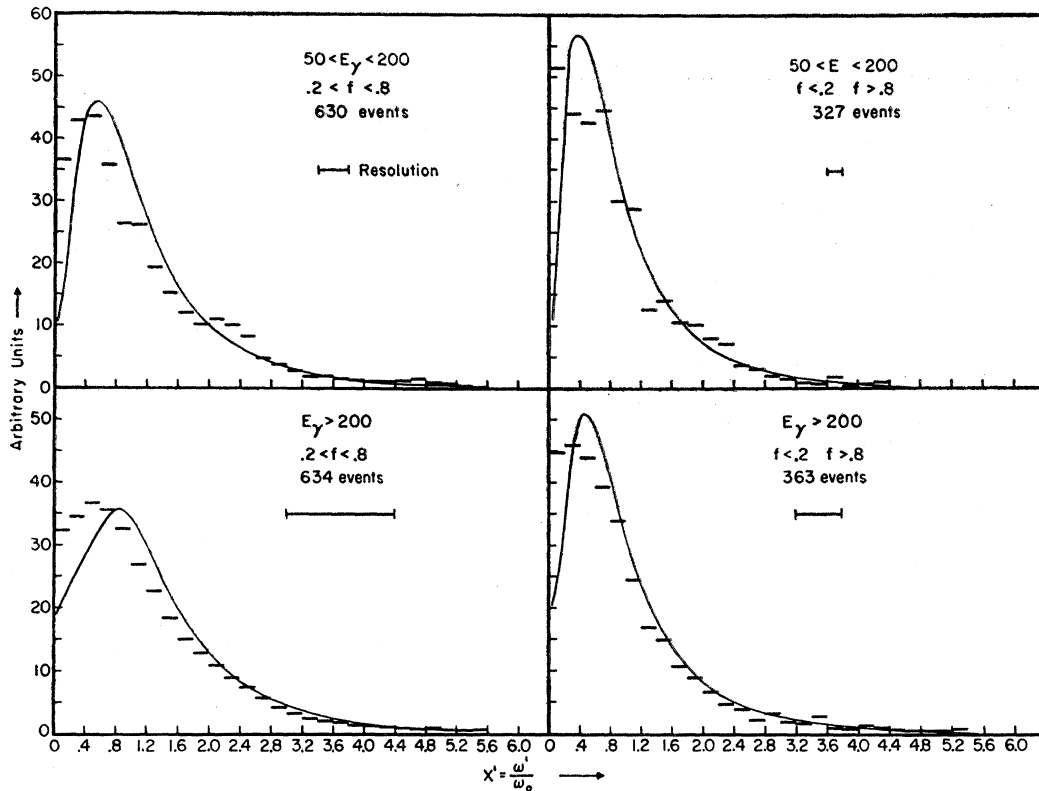


FIG. 7. Distribution of the projected opening angle, ω' , between the members of electron pairs, for two photon energy intervals and for two groups of events having roughly even and uneven sharing of the incoming energy. The solid curves are the theoretical distributions as deduced from Borsellino's equations.⁷ An angular resolution of $\pm \frac{1}{4}^\circ$ is folded into the theoretical curves. On the abscissa is plotted $x' = \omega'/\omega_0$, where $\omega_0 = mc^2 E_\gamma / (E^+ E^-)$.

estimate of E_γ , given the opening angle ω , when no information on f is available.

Our data, grouped in two photon energy intervals, irrespective of the value of f , give the following results:

$$50 < E_\gamma < 200 \text{ Mev}, \quad \phi_{\text{med}} = 1.54 \pm 0.07;$$

$$200 < E_\gamma < 1040 \text{ Mev}, \quad \phi_{\text{med}} = 1.67 \pm 0.10.$$

Since ϕ_{med} appears to be practically energy independent, a value $\phi_{\text{med}} = 1.7$ can be used well above 1 Bev.

VIII. CONCLUSIONS AND ACKNOWLEDGMENTS

Our results may be summarized as follows:

(a) For E.F. pairs the shape of the momentum distribution of the recoil electron is in good agreement with the distribution predicted by Suh and Bethe in the region of validity of their calculations, i.e., $E_\gamma > \sim 100$ Mev. For $10 < E_\gamma < 100$ Mev the results indicate that Suh and Bethe's distribution still describe the data at least for $q_R < \sim 1$ Mev/c.

(b) The partial cross sections $\sigma_{\text{E.F.}}(q_R \geq 0.15 \text{ Mev}/c)$ and $\sigma_{\text{E.F.}}(q_R \geq 0.02 \text{ Mev}/c)$ predicted by Suh and Bethe are consistent with the total cross section for E.P. pairs predicted by Wheeler and Lamb in the region $100 < E_\gamma < 1000$ Mev.

(c) The total cross section for E.F. pair production at photon energies between 10 Mev and 100 Mev is consistent with the Wheeler-Lamb calculation.

(d) The energy partition between the electron and the positron for both E.F. and P.F. pairs is in agreement with the Bethe-Heitler theory.

(e) The measured distribution of the opening angle between pair members of P.F. and E.F. pairs is in agreement with Borsellino's theoretical results for $x' > \sim 1.5$ but appears to be shifted toward lower values when x' is small. The median values of x for the experimental distributions are 10 to 20% lower than those for the corresponding theoretical curves.

Finally, information is provided on the angular distribution of the recoil electrons, for which there is no theoretical prediction.

The diffusion cloud chamber has proved to be an excellent instrument for this type of research. For photon energies below a hundred Mev, the efficiency for detecting E.F. pairs is very close to 100%, and at 1 Bev is still $\sim 75\%$.

We are indebted to Dr. Bethe, Dr. Borsellino, Dr. Rohrlich, Mr. Suh, and Mr. Malamud for several useful discussions. We want to thank Dr. K. Greisen and Dr. K. Rogers for collaboration in the early

developments of this experiment; Mrs. Louise Van Nest for help in the measurements; and the Laboratory staff and synchrotron crew for assistance in the operation of the accelerator.

IX. APPENDIX. EFFECT OF THE LiH HARDENER ON THE BREMSSTRAHLUNG BEAM

For experimental purposes it is of interest to examine the modifications undergone by a bremsstrahlung beam when passed through a LiH hardener.

Our data refer to the photon beam produced by 1040-Mev electrons striking a thin tungsten target, and to a hardener consisting of 2.65 radiation lengths (~ 4 meters) of LiH. The collimator in front of the chamber subtended an angle of $\sim 1/100$ rad at the end of the LiH pipe.

The momentum measurements described in Sec. 6 provide direct information on the number of pairs and triplets produced by the beam, as a function of the photon energy. A total of 3065 events were available for this analysis.

The photon spectrum is deduced by assuming that both the P.F. and E.F. pair cross sections are described by the Wheeler and Lamb formulas. The histogram of Fig. 8 is obtained by dividing the number of events observed in each energy interval by the total cross section ($\sigma_{E.F.} + \sigma_{P.F.}$) averaged over that interval. It represents the photon spectrum crossing the chamber. The solid curve is the theoretical thin-target bremsstrahlung spectrum. The scales are chosen so that the number of photons in any interval between 1 Mev and 1040 Mev is proportional to the area of that interval.

In comparison to the thin-target spectrum, the essential features of the hardened beam are the following:

1. The ratio of the number of photons between 100 and 300 Mev to the number between 300 and 1040 Mev

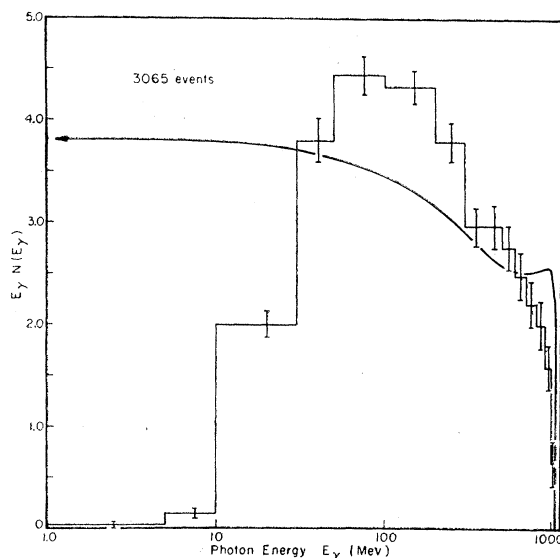


FIG. 8. Effect of the LiH hardener on the bremsstrahlung spectrum. The solid line is the theoretical thin-target bremsstrahlung spectrum. The histogram describes the spectrum hardened by 2.6 radiation lengths of LiH, i.e., the spectrum crossing the cloud chamber. The two curves are normalized so that, for equal total energy in the beam (equal Q 's), the ratio of the ordinates is equal to the ratio of the intensities, for any value of E_γ .

is ~ 1.4 , while it is ~ 1.1 for the thin-target spectrum. Possibly this ratio can be reduced by better collimation of the beam entering the detector, or by decreasing somewhat the length of the hardener.

2. Photons with energies below 10 Mev are practically absent. This feature is essential for the use of a diffusion (or bubble) chamber as a target-detector in a bremsstrahlung beam: without the hardener, the background caused by the photons at the low-energy end of the spectrum would be prohibitive.

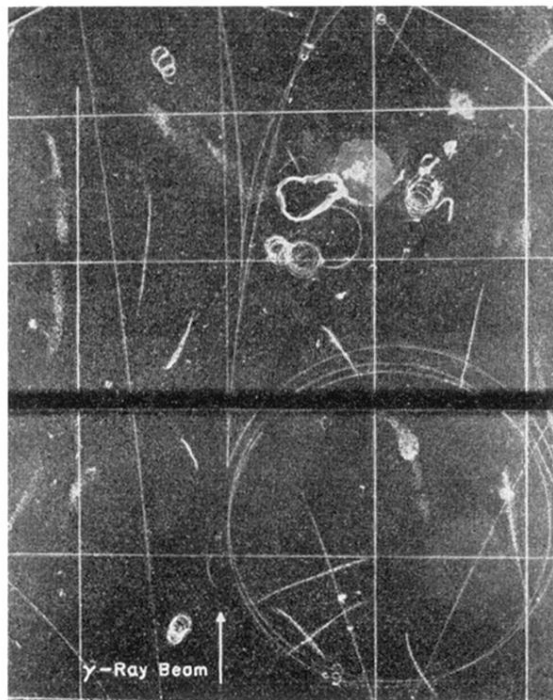


FIG. 2. Examples of events observed in the cloud chamber. The event in the upper half of the picture is a pair produced in the field of a proton by a photon of 97 Mev. The other event is a pair produced by a photon of 620 Mev in the field of an electron which recoils with a momenta of $9.8 \text{ Mev}/c$.